Turkish J. Eng. Env. Sci.
34 (2010) , 17 – 24.

doi:10.3906/muh-0910-57

Effect of layer angle on tensile behavior of oblique layer functionally graded steels

Ali NAZARI, Shadi RIAHI
Department of Technical and Engineering Sciences, Islamic Azad University (Saveh Branch), IRAN
e-mail: alinazari84@aut.ac.ir

Received 20.10.2009

Abstract

In this work, tensile and yield stress and tensile and yield strain of oblique layer functionally graded steels produced by electroslag remelting were investigated. Functionally graded steels containing ferrite, austenite, bainite, and/or martensite layers may be fabricated via diffusion of alloying elements during the remelting stage. Tensile and yield stress and tensile and yield strain of functionally graded steels depend on the composition, containing layers, and angles of oblique layers. By increasing the angle of layers with respect to the load axis, the tensile and yield stresses of functionally graded steels were decreased.

Key Words: Functionally graded steels, Tensile test, Oblique layer

Introduction

There exists a wide variety of applications in engineering practice in which variations in strength appear: for instance, in welded structures, soldered joints, and nitrided or case-hardened components. In all structures consisting of multiphase materials, composites, or graded materials, strength variations are inherent. The first experimental evidence that a gradient in strength influences the behavior of cracks was found by Suresh et al. (1992). They conducted fatigue experiments on an explosion-clad bimaterial consisting of a ferritic steel and an austenitic steel. For a crack approaching the interface from the softer ferritic steel (a soft-hard transition), the crack growth rate dropped precipitously and the crack stopped some distance before the interface. In contrast, for a crack approaching the interface from the harder austenitic steel (a hard-soft transition), the crack advanced through the interface. The crack growth rate remained roughly constant, except for some distance before the interface, where a slight increase of the crack growth rate was noted.

A practical application of this experimental finding has been reported by Suresh et al. (1993). To rationalize the yield stress gradient effect, Sugimura et al. (1995) conducted finite element computations. They considered stationary, monotonically loaded cracks at various distances, t, from a bimaterial interface. The elastic constants were the same for both materials but the plastic properties differed. The results demonstrated that the near-tip crack driving force deviates from the far-field value when the crack approaches the interface.

Kim et al. (1997) have compared the yield stress gradient effect in a bimaterial to that in a bimaterial with interlayers. Kolednik (2000) provided an analytical model to explain why gradients in yield stress affect the crack growth behavior. It was demonstrated that a yield stress gradient induces an additional term of the crack driving force, which leads to an increase or decrease of the effective crack driving force.

Becker et al. (2002) modeled fracture toughness measured by a single edge-crack tension (SE(T)) specimen, with cracks perpendicular to and along the strength gradient, and a homogeneous Young's modulus using Weibull statistics. Bezensek and Hancock (2007) studied the fracture toughness and Charpy impact resistance of functionally graded steels (FGSs) produced by laser welding. A method of creating a functionally graded structural member by transforming its material at cryogenic temperatures has been presented by Skoczen (2007), by imposing kinematically controlled torsion on a stainless steel bar until the phase transformation threshold was reached and the material began transforming itself close to the outside radius of the bar.

Another type of FGS with strength gradient, produced from austenitic stainless steel and carbon steel using electroslag refining (ESR), was investigated by Aghazadeh and Shahosseinie (2005). By selecting the appropriate arrangement and thickness of original ferritic ($\dot{\alpha}$) and original austenitic ($\dot{\gamma}$) steels as electrodes, they could obtain composites with several layers, consisting of ferrite, austenite, bainite, and martensite. Formation of the bainitic and martensitic layers for the 3-layer resultant composite is as ;ollows:

$$(\dot{\alpha}\dot{\gamma})_{el} \xrightarrow{R} (\alpha\beta\gamma)_{com}$$

$$(\dot{\gamma}\dot{\alpha}\dot{\gamma})_{el} \xrightarrow{R} (\gamma M\gamma)_{com}$$

where; $\alpha\beta$, γ, and M are the ferrite, austenite, bainite, and martensite layers in the final composite, respectively; el is electrode; com is composite; and R is remelting.

The diffusion of chromium, nickel, and carbon atoms taking place at the remelting stage in the liquid phase controls the chromium, nickel, and carbon atom distribution patterns (Figures 1a and 1b) in the produced composites (Aghazadeh and Shahosseinie, 2005). The thicknesses of the bainitic (Figure 1a) and martensitic (Figure 1b) layers depend on the thickness of the primary electrodes and process variables (voltage, current intensity, and the drawing velocity of the product) and were similar for all produced composites. In Figures 2a and 2b, the microstructure of the bainite layer formed between the ferritic and austenitic regions, and the martensite layer formed between the 2 austenitic regions, are illustrated, respectively (Aghazadeh et al., 2005, 2006; Nazari and Aghazadeh, 2009, 2010). Transformation characteristics (Aghazadeh and Shahosseinie, 2005), tensile properties (Aghazadeh et al., 2006), and Charpy impact energy (Nazari and Aghazadeh, 2009, 2010) of FGSs have been fully discussed previously.

Unquestionably, there exist several applications in which the direction of the load axis is not parallel to the laminal interface. Under such conditions, the load regime would considerably differ in the specimen. In fact, in most cases, we encountered such situations, and the investigation of these conditions is inherent. Thus, in this work, the tensile and yield stress and tensile and yield strain of FGSs with oblique layers have been investigated. It has been shown that the composition, containing layers, and angle of oblique layers change the tensile behavior; as was expected; by increasing the angle of layers with respect to the load axis, tensile and yield stresses were decreased.

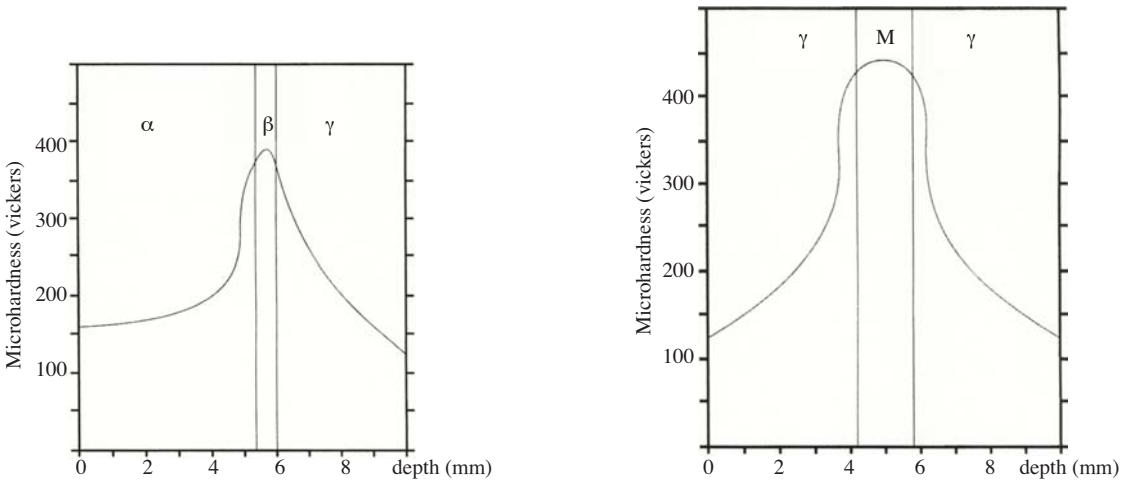

Figure 1. Vickers microhardness profile versus depth in (a) $\alpha\beta\gamma$ and (b) $\gamma M\gamma$ composites.

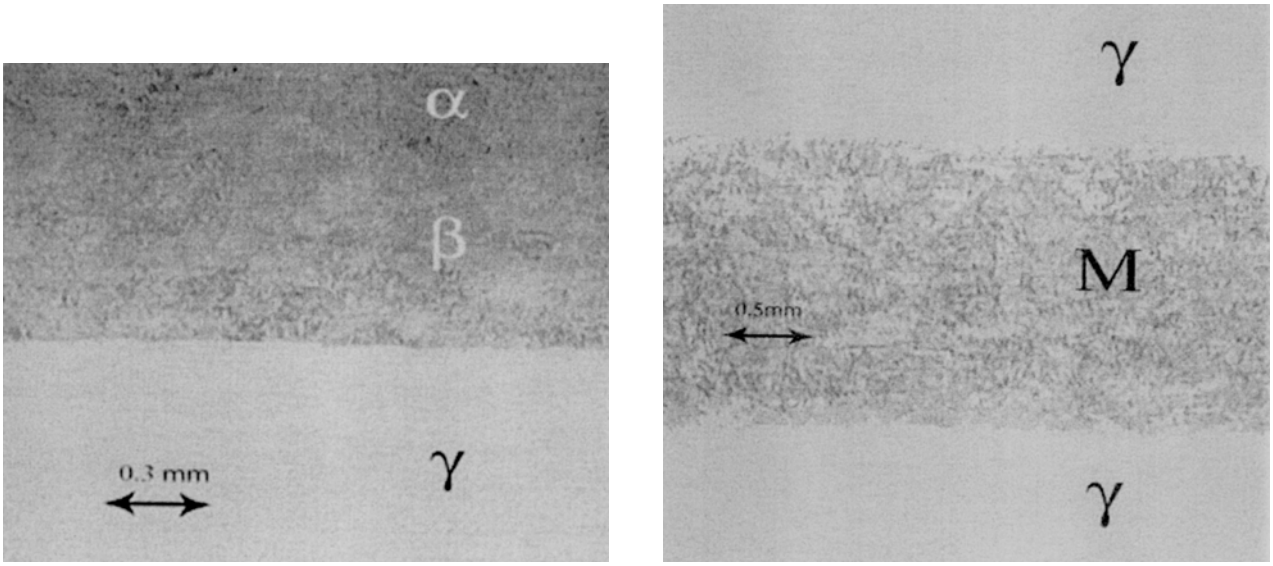

Figure 2. The microstructure of (a) the bainite layer formed between alpha and gamma and (b) the martensite layer formed between 2 layers of gamma steel.

Experimental Procedure

Similar to previous works (Aghazadeh et al., 2005, 2006; Nazari and Aghazadeh, 2009, 2010), to make FGSs, a miniature ESR apparatus was used. The consumed slag was a mixture of 20% CaO, 20% Al_2O_3, and 60% CaF_2. The original ferritic and austenitic steel rods that were employed as electrodes were commercial-type AISI 1020 and AISI 316 steels, respectively, and their chemical compositions are given in Table 1.

Table 1. Chemical composition of original ferrite and austenite steels.

	%C	%Si	%Mn	%P	%S	%Cr	%Ni
$\dot{\gamma}$	0.07	1	2	0.045	0.03	18.15	9.11
$\dot{\alpha}$	0.2	0.3	0.2	0.05	0.05	-	-

Different arrangements of ferritic and austenitic steel slices were spot welded for remelting in the form of 2- and 3-piece electrodes. The thickness of each slice in the primary electrode is illustrated in Table 2. The diameter of the steel rods was 65 mm. Since the contribution of all layers in the gauge of a tensile specimen is necessary, 2 auxiliary electrodes were spot welded to the top and bottom side of the composite in accordance to the type of the top or bottom layer (i.e. an auxiliary $\dot{\alpha}$ slice for the sides with an $\dot{\alpha}$ layer and an auxiliary $\dot{\gamma}$ slice for the sides with a $\dot{\gamma}$ layer).

Table 2. Thickness of utilized slices of primary electrodes together with the thickness of bainite and martensite layers in forged composite specimens (mm).

		15°	30°	45°	60°	75°
$\alpha\beta\gamma$ composites	Original electrode slices	30		50		
γMγ composites	Outside slice	18.7		31.2		
	Middle slice	22.5		37.5		
Auxiliary electrodes		90		150		
Thickness of bainite layer		0.5	0.8	1.1	1.3	1.5
Thickness of martensite layer		1.2	2.1	2.9	3.4	3.8
Thickness of forged composite		27	51	74.5	87	97

$\alpha\beta\gamma$ and γMγ composites were produced from $\dot{\alpha}\dot{\gamma}$ and $\dot{\gamma}\dot{\alpha}\dot{\gamma}$ electrodes, respectively, in accordance with previous works (Aghazadeh et al., 2005, 2006; Nazari and Aghazadeh, 2009, 2010). Electroslag remelting experiments were carried out under a constant power supply of 16 KVA. After remelting, the composite ingots were hot-pressed down to the thicknesses listed in Table 2 and a diameter of 90 mm. The hot-pressing was done at 980 °C and then the specimens were air-cooled. The thickness of utilized slices to produce tensile test specimens with angles of 15° and 30° with respect to the load axis was different from the other specimens, because by selecting thicknesses similar to the other composites, the total reduction was too large and might have resulted in failing the specimens.

Tensile tests were carried out under an extension rate of 0.1 mm/s. The specimens' dimensions were in accordance with the ASTM E8 standard and are shown in Figure 3. Figure 3 also shows that the tensile test specimens were prepared such that the gauge consisted of functionally graded layers positioned in an oblique manner toward the load axis. Tensile test specimens from received alpha and gamma steel rods were prepared after annealing at 980 °C and subsequent air-cooling. To acquire tensile behavior of the bainite and martensite layers, tensile specimens of the same composition and same mechanical properties as the bainitic and martensitic layers were produced, similar to previous studies (Aghazadeh et al., 2006; Nazari and Aghazadeh, 2009, 2010). Initially, the average chemical composition of the bainite and martensitic layers was obtained (Table 3). Afterwards, the bainitic and martensitic samples with chemical composition in accordance with the average chemical composition of the bainitic and martensitic layers were produced by means of a vacuum induction furnace. Similar to the primary composites, the hot rolling process was carried out at 980 °C, followed by air-cooling. Through trial and error (i.e. conforming the chemical composition and changing the cooling rate), the samples with the microhardness closest to that of the bainitic and martensitic layers were selected and tensile test specimens from the bainitic and martensitic samples were made.

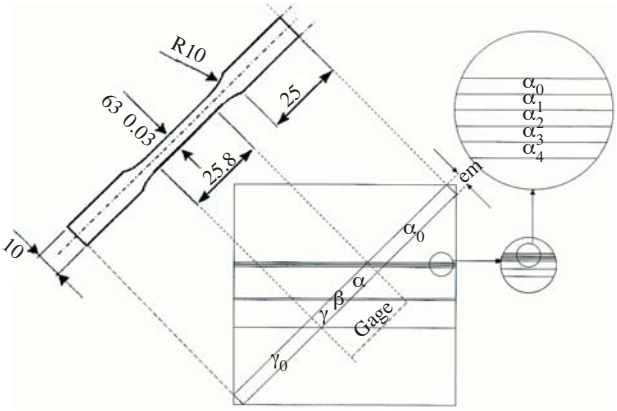

Figure 3. Schematic illustration of the method utilized for preparation of tensile test specimens together with tensile specimens' dimensions (mm).

Table 3. Chemical composition (wt. %) of bainitic and martensitic layers together with the single-phase bainite and martensite specimens produced from samples.

Specimen studied	% Cr	% Ni	% C	% Si	% Mn	% S	% P
Single-phase bainite	14.5	7.2	0.12	0.8	1.8	0.03	0.04
Bainite specimen produced from the sample	14.7	7.15	0.13	0.85	1.9	0.032	0.045
Single-phase martensite	7.3	3.2	0.19	0.39	0.3	0.04	0.05
Martensite specimen produced from the sample	7.38	3.14	0.21	0.28	0.28	0.033	0.055

Results and Discussion

Metallographic studies from the cross section of the produced composites show that the new stabilized phases in all composites produced under similar conditions have similar features; the thickness of the martensite layer and that of the bainite layer, which were verified by the Vickers microhardness examination, are in accordance with previous works (Aghazadeh et al., 2005, 2006; Nazari and Aghazadeh, 2009, 2010). The graded nature of the produced composites was verified using the Vickers microhardness and carbon, nickel, and chromium concentration profiles, which are fully discussed in previous works (Aghazadeh et al., 2005, 2006). The Vickers microhardness profile of the tensile specimens with layers parallel to the load direction with a thickness of 10 mm is illustrated in Figures 1a and 1b (Aghazadeh and Shahosseinie, 2005).

Tensile and yield stress and tensile and yield strain of oblique layer functionally graded steels are given in Table 4. For comparison, the stress-strain curves of original ferrite, original austenite, and single-phase bainite and martensite are shown in Figure 4 (Nazari and Aghazadeh, 2009, 2010). By increasing the angle of layers with respect to the load axis, tensile and yield stresses decrease, together with the yield strain of the composites, while the tensile strain of the composites increases.

To investigate tensile behavior of each oblique layer of $\alpha\beta\gamma$ composites, the composite may be considered as a combination of an alpha region with m_α oblique layers, a bainite layer, and a gamma region with $n_\gamma$oblique layers. First, consider the situation in which the layers are placed at an oblique 45° with respect to the load axis. We are able to divide the layers into square elements, according to Figure 5. The elements labeled γ_0 to γ_i in row 1 experience the same strain level. On the other hand, the elements labeled γ_i to α_0 in column 1 experience the same stress level. When the specimen has undergone tensile load, the elements that are placed

Table 4. Yield and tensile stress and yield and tensile strain of produced composites.

Angle of layers	$\alpha\beta\gamma$				$\gamma M\gamma$			
	(a)	(b)	(c)	(d)	(a)	(b)	(c)	(d)
15°	371	0.002	559	0.19	383	0.003	653	0.05
30°	418	0.005	581	0.23	425	0.007	708	0.07
45°	568	0.009	693	0.31	896	0.013	935	0.17
60°	772	0.012	856	0.29	1011	0.019	1097	0.15
75°	824	0.018	897	0.26	1042	0.027	1121	0.10

(a) Yield stress (MPa) (b) Yield strain (c) Tensile stress (MPa) (d) Tensile strain

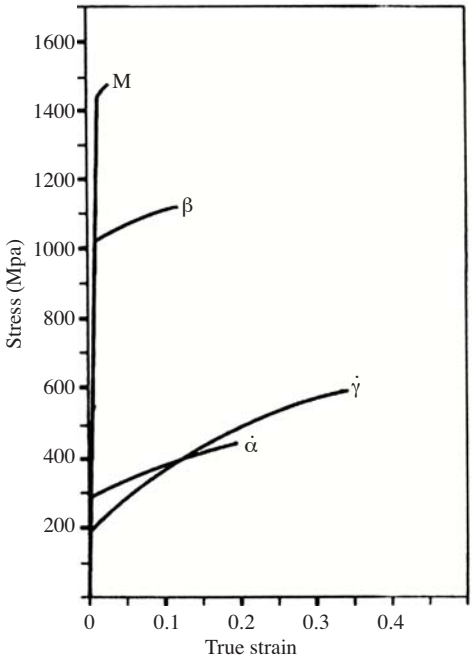

Figure 4. Stress-strain curve of original ferrite, original austenite, single-phase bainite, and martensite specimens.

in row 1 do not flow until the γ_i element flows. Because the γ_i and γ_{i+1} elements experience the same stress level, after the flowing of the γ_i element, the elements that lie in row 2 flow by controlling the γ_{i+1} element. This condition continues in the same manner until the bainite layer flows. Therefore, the layer with the highest yield stress (the bainite layer in the $\alpha\beta\gamma$ composite) controls the total specimen yielding (i.e. the yielding of all specimen layers completed after the yielding of the bainite layer). The yielding of the composite begins with the flowing of row 1 and could be determined by considering all constituent layers. For the case of the specimen with layers parallel to the load axis, all of the layers in the total length of the specimen simultaneously yield. Thus, the yield stress of this specimen is the highest because of the much higher volume fraction contribution of the layers in the composite yielding. For the tensile specimen with layers normal to the load axis, because all layers experience the same stress level, the yielding of the composite is controlled by the layer with the lowest yield strain (i.e. the original austenite layer). Since a combination of same stress levels (for elements placed in a given column) and same strain levels (for elements placed in a given row) is available, the composite flows until the strain of the specimen reaches the tensile strain of the original ferrite layer. Thus, the layer with the lowest tensile stress (i.e. the original ferrite layer) controls the fracture of the composite. Keeping in mind that

the original ferrite layer has the maximum tensile strain in the composite and that failure of this layer leads to composite fracture, the tensile strain of the composite should be different from that of the original ferrite layer, because the tensile strains of all the layers contribute to the tensile strain of the composites. According to the tensile stress and tensile strain of each layer, the tensile stress of each layer that contributes to the tensile strength of the composite could be determined using the stress-strain curve of each element.

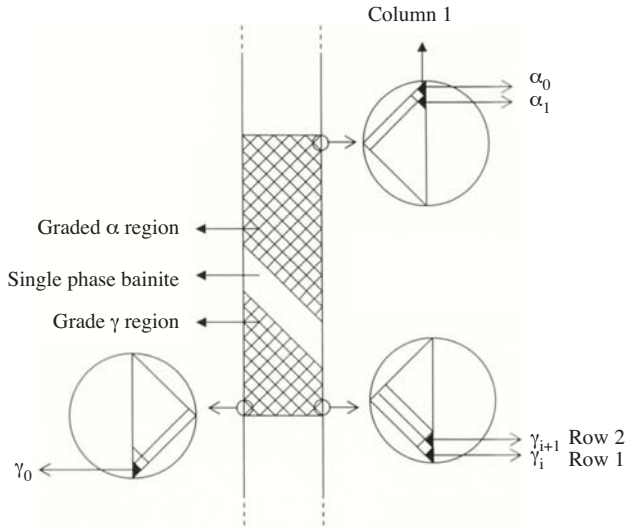

Figure 5. Schematic illustration of square elements in the tensile specimen with layers at an angle of 45° with respect to the load axis.

Although for angles other than 45° one could not completely discuss the tensile behavior of the specimens based on the above observations, the tensile behavior of the specimens could be justified approximately. Yield and tensile stresses for composites with layers at angles of 15° and 30° with respect to the load axis, in comparison to those with layers at angles of 45°, 60°, and 75° with respect to the load axis, are relatively low. The values of yield and tensile stresses for specimens with lower angle layers (i.e. 15° and 30°) do not have large differences with respect to composites with layers at higher angles (i.e. 45°, 60 °, and 75°). This may be due to the fact that the isostress behavior of the elements with lower angles is the majority mechanism. Therefore, when the composites are loaded, layers with lower yield and tensile stresses flow so much that the contribution of layers with higher yield and tensile stresses (i.e. martensite and bainite) in the yield and tensile stresses of the composites is inconsequential. For this reason, the tensile strain of composites containing lower angle layers is relatively large with respect to that of the composites containing higher angle layers, unlike the yield strain, which is less. On the other hand, the yield and tensile strains of the composites containing layers at angles of 45° are higher than those of the other composites. For specimens with angles lower than 45°, the contribution of the layers in plastic deformation is low, and for angles higher than 45°, this contribution is high. Thus, based on the rule of mixtures, the strains of the composites reach a maximum in the composite containing layers of 45° with respect to the load axis.

For γMγ composites, a similar discussion could be followed. In fact, the tensile behavior of all composites depends on the layer of angles in a specific composite (i.e. $\alpha\beta\gamma$ and γMγ composites).

Conclusions

From the above discussion, it may be concluded that:

1. Yield and tensile stress and yield and tensile strain of oblique layer functionally graded steels depended on the composition, containing layers, and angle of oblique layers.

2. Yield and tensile strains of the composites containing the layer angle of 45° were higher than those of the other composites.

3. The effect of layers with high strength and low tensile strain (i.e. bainite and martensite) on the final tensile and yield stress and tensile and yield strain for composites containing low angle layers with respect to the load axis was unimportant.

References

Aghazadeh, J.M. and Shahosseinie, M.H., "Transformation Characteristics of Functionally Graded Steels Produced by Electroslag Remelting", Metallurgical and Materials Transactions A, 36A, 3471-3476, 2005.

Aghazadeh, J.M., Shahosseinie, M.H. and Parastar Namin, R., "Tensile Behavior of Functionally Graded Steels Produced by Electroslag Remelting", Metallurgical and Materials Transactions A, 37A, 2125-2132, 2006.

Becker, T.L. Jr, Cannon, R.M. and Ritchie, R.O., "Statistical Fracture Modeling: Crack Path and Fracture Criteria with Application to Homogeneous and Functionally Graded Materials", Engineering Fracture Mechanics, 69, 1521-1555, 2002.

Bezensek, B. and Hancock, J.W., "The Toughness of Laser Welded Joints in the Ductile-Brittle Transition", Engineering Fracture Mechanics, 74, 2395-2419, 2007.

Kim, A.S., Suresh, S. and Shih, C.F., "Plasticity Effects on Fracture Normal to Interfaces with Homogeneous and Graded Compositions", International Journal of Solids and Structures, 34, 3415-3432, 1997.

Kolednik, O., "The Yield Stress Gradient Effect in Inhomogeneous Materials", International Journal of Solids and Structures, 37, 781-808, 2000.

Nazari A. and Aghazadeh J.M., "Impact Energy of Functionally Graded Steels with Crack Divider Configuration", Journal of Materials Science and Technology, 25, 847-852, 2009.

Nazari A. and Aghazadeh J.M., "Impact Energy of Functionally Graded Steels in Crack Divider Configuration", Journal of Materials Engineering and Performance, DOI: 10.1007/s11665-009-9578-4, 2010.

Skoczen, B., "Functionally Graded Structural Members Obtained Via the Low Temperature Strain Induced Phase Transformation", International Journal of Solids and Structures, 44, 5182-5207, 2007.

Sugimura, Y., Lim, P.G., Shih, C.F. and Suresh S., "Fracture Normal to a Bimaterial Interface: Effects of Plasticity on Crack-Tip Shielding and Amplification", Acta Metallica Materialia, 43, 1157-1169, 1995.

Suresh, S., Sugimura, Y. and Ogawa T., "Fatigue Cracking in Materials With Brittle Surface Coatings" Scripta Metallurgica, 29, 237-242 , 1993.

Suresh, S., Sugimura, Y. and Tschegg E., "The Growth of a Fatigue Crack Approaching a Perpendicularly-Oriented, Biomaterial Interface", Scripta Metallurgica, 27, 1189-1194, 1992.